

Sensing Rate Optimization for Multi-Band Cooperative ISAC Systems

Nemanja Stefan Perović, Mark F. Flanagan, *Senior Member, IEEE*, and Le-Nam Tran, *Senior Member, IEEE*

Abstract—Integrated sensing and communication (ISAC) has been recognized as one of the key technologies for future wireless networks, which potentially need to operate in multiple frequency bands to satisfy ever-increasing demands for both communication and sensing services. Motivated by this, we consider the sum sensing rate (SR) optimization for a cooperative ISAC system with linear precoding, where each base station (BS) works in a different frequency band. With this aim, we propose an optimization algorithm based on the semi-definite rank relaxation that introduces covariance matrices as optimization variables, and we apply the inner approximation (IA) method to deal with the nonconvexity of the resulting problem. Simulation results show that the proposed algorithm increases the SR by approximately 25 % and 40 % compared to the case of equal power distribution in a cooperative ISAC system with two and three BSs, respectively. Additionally, the algorithm converges in only a few iterations, while its most beneficial implementation scenario is in the low power regime.

Index Terms—Cooperative, communication rate (CR), integrated sensing and communication (ISAC), multi-band, sensing rate (SR).

I. INTRODUCTION

In addition to conventional communication services, future sixth-generation (6G) communication systems will need to provide high-precision sensing as a new necessary functionality underpinning different applications (e.g., augmented reality, digital twins). A promising technology for the implementation of this functionality with minimal additional resource usage is that of integrated sensing and communication (ISAC) [1]. This refers to a design paradigm in which sensing and communication systems are integrated to efficiently utilize the shared spectrum and hardware resources, while offering mutual benefits [2]. As such, ISAC is expected to be one of the key technologies in sixth-generation (6G) networks, which offers flexible trade-offs between the two functionalities across various use cases.

With the rise of high-data rate applications, wireless traffic demand is sharply increasing. This leads to spectrum congestion in the radio frequency (RF) band, which is insufficient for higher rate services. To meet these demands, all available spectrum, including sub-6 GHz, millimeter-wave (mmWave) and terahertz (THz) bands, must be fully utilized [3]. Furthermore, high-frequency technology also enables advanced sensing and localization with centimeter-level accuracy. Hence, frequency

resource allocation is crucial for supporting both communication and sensing demands. Ultimately, future wireless networks will operate simultaneously in different frequency bands and will also need to possess cooperative capabilities. This fact motivates the development of cooperative ISAC systems that simultaneously operate in more than one frequency band.

Recent studies have explored ISAC in cooperative communication systems. A joint base station (BS) mode selection, transmit beamforming, and receive filter design for cooperative cell-free ISAC networks, where multiple BSs cooperatively serve communication users and detect targets, were studied in [4]. In [5], stochastic geometry was used to analyze scaling laws in cooperative ISAC networks, and it was shown that the sensing performance increases significantly with the number of ISAC transceivers, especially when all ISAC transceivers are equidistant from the target. In [6], a maximum likelihood (ML) framework for target localization was developed, deriving a cooperative position error bound (PEB) for the networked orthogonal time frequency space (OTFS)-based system which serves as a lower bound on the positioning accuracy. Performance analysis and optimal power allocation in a cooperative ISAC system with a micro and a macro BS, where the micro BS performs sensing and acts as a full-duplex relay, were presented in [7].

In contrast to existing studies on cooperative ISAC in a single frequency band, multi-band cooperative ISAC remains largely unexplored. In [8], a relatively complex method for fusion of orthogonal frequency division multiplexing (OFDM) sensing signals from different bands was proposed which achieved high-accuracy target localization, requiring dual-band processing at both BSs. A similar approach but for single-BS ISAC in [9] improved the sensing Cramer-Rao lower bound (CRLB) and communication mutual information (MI), though it did not account for propagation loss differences between frequency bands.

Against this background, the contributions of this paper are listed as follows:

- We extend the MI framework developed in [10] to a multi-band cooperative ISAC system, where each BS operates in a different frequency band. To maximize the sum sensing rate (SR) for this system, we formulate a joint optimization problem of the transmit precoding matrices. For this purpose, we adopt linear precoding. To maintain user fairness, each user has a guaranteed minimum communication rate (CR).
- We solve the considered problem by employing the semi-definite rank relaxation method, which aims to find the covariance matrices of the corresponding precoding matrices. The inner approximation (IA) method is applied to deal with the nonconvexity of the resulting problem.

Nemanja Stefan Perović was with Université Paris-Saclay, CNRS, CentraleSupélec, Laboratoire des Signaux et Systèmes, 3 Rue Joliot-Curie, 91192 Gif-sur-Yvette, France. He is now with the Institute of Communications Engineering, National Sun Yat-sen University, Kaohsiung 80424, Taiwan, R.O.C. (Email: n.s.perovic@mail.nsysu.edu.tw).

Mark F. Flanagan and Le-Nam Tran are with the School of Electrical and Electronic Engineering, University College Dublin, Belfield, Dublin 4, D04 V1W8, Ireland (Email: mark.flanagan@ieee.org, nam.tran@ucd.ie).

- We demonstrate through simulations that the proposed algorithm *increases the SR by approximately 25 % and 40 %* compared to the case of equal power distribution in a cooperative ISAC system with two and three BSs, respectively. Additionally, the algorithm converges in a couple of iterations. Moreover, we show that the operating frequency and the distance from the sensing target have a significant impact on the SR. Lastly, we conclude that the most preferred application scenario for our proposed system model is in the low power regime.

Notation: Bold lower and upper case letters represent vectors and matrices, respectively. \mathbf{I}_x is the unit matrix of size $x \times x$. $\text{Tr}(\mathbf{X})$, $\text{vec}(\mathbf{X})$, $\det(\mathbf{X})$ and $\text{rank}(\mathbf{X})$ denote the trace, vectorization, determinant and rank of matrix \mathbf{X} , respectively. $\ln(\cdot)$ is the natural logarithm and \otimes denotes the Kronecker product. $(\cdot)^*$ denotes complex-conjugate. $(\cdot)^T$ and $(\cdot)^H$ represent transpose and Hermitian transpose, respectively.

II. SYSTEM MODEL AND PROBLEM FORMULATION

We consider a system with B BSs, each being equipped with N_t transmit and N_r receive antennas, simultaneously serving K communication users and performing target sensing. Each BS operates on a different frequency band. A BS $b \in \mathcal{B} \triangleq \{1, 2, \dots, B\}$ operates at center frequency $f^{(b)}$, corresponding wavelength $\lambda^{(b)}$, and bandwidth $B^{(b)}$. Each user $k \in \mathcal{K} \triangleq \{1, 2, \dots, K\}$ has N_k antennas. Data symbols of unit average power are transmitted over the period of L time slots and are denoted as $\mathbf{S}^{(b)} = [(\mathbf{S}_1^{(b)})^T, (\mathbf{S}_2^{(b)})^T, \dots, (\mathbf{S}_K^{(b)})^T]^T$, where $\mathbf{S}_k^{(b)} \in \mathbb{C}^{N_k \times L}$ represents data symbols transmitted to user k and $N_{\text{tot}} = \sum_{k=1}^K N_k$. For asymptotically large L , we have

$$\mathbf{S}^{(b)}(\mathbf{S}^{(b)})^H \approx L\mathbf{I}_{N_{\text{tot}}}. \quad (1)$$

To provide high-quality communication and sensing links, data for the k -th user is precoded using $\mathbf{W}_k^{(b)} \in \mathbb{C}^{N_t \times N_k}$. At low-frequency bands, fully digital precoding is applied, while at high-frequency bands, a hybrid precoding scheme is employed with $\mathbf{W}_k^{(b)} = \mathbf{W}_{RF,k}^{(b)} \mathbf{W}_{BB,k}^{(b)}$, where $\mathbf{W}_{BB,k}^{(b)} \in \mathbb{C}^{N_k \times N_k}$ is the fully digital baseband precoder and $\mathbf{W}_{RF,k}^{(b)} \in \mathbb{C}^{N_t \times N_k}$ as the analog precoder implemented using RF phase shifters. Hence, all of the elements of $\mathbf{W}_{RF,k}^{(b)}$ must satisfy

$$|\mathbf{W}_{RF,k}^{(b)}(i, j)| = 1, \quad i = 1, 2, \dots, N_t, j = 1, 2, \dots, N_k. \quad (2)$$

After precoding, the transmitted signal can be written as

$$\mathbf{X}^{(b)} = \mathbf{W}^{(b)} \mathbf{S}^{(b)} = \sum_{k=1}^K \mathbf{W}_k^{(b)} \mathbf{S}_k^{(b)} \in \mathbb{C}^{N_t \times L} \quad (3)$$

where $\mathbf{W}^{(b)} = [\mathbf{W}_1^{(b)}, \mathbf{W}_2^{(b)}, \dots, \mathbf{W}_K^{(b)}] \in \mathbb{C}^{N_t \times N_{\text{tot}}}$.

A. Communication Model

For the frequency band b , the received signals of all users can be stacked to form a matrix $\mathbf{Y}_C^{(b)}$, given by

$$\mathbf{Y}_C^{(b)} = \mathbf{H}^{(b)} \mathbf{X}^{(b)} + \mathbf{N}^{(b)} \in \mathbb{C}^{N_{\text{tot}} \times L} \quad (4)$$

where $\mathbf{H}^{(b)} = [\mathbf{H}_1^{(b)T}, \mathbf{H}_2^{(b)T}, \dots, \mathbf{H}_K^{(b)T}]^T \in \mathbb{C}^{N_{\text{tot}} \times N_t}$ with $\mathbf{H}_k^{(b)} \in \mathbb{C}^{N_k \times N_t}$ being the channel matrix between the b -th

BS and the k -th user. $\mathbf{N}^{(b)} \in \mathbb{C}^{N_{\text{tot}} \times L}$ is the noise matrix consisting of independent and identically distributed (i.i.d.) elements that are distributed according to $\mathcal{CN}(0, (\sigma^{(b)})^2)$. Assuming a sparsely-scattered channel model, the channel matrix can be expressed as

$$\mathbf{H}_k^{(b)} = \sqrt{\frac{N_t N_k}{P^{(b)}}} \sum_{p=1}^{P^{(b)}} \beta_{p,k}^{(b)} \mathbf{a}_R(\theta_{p,k}^{(b)}) \mathbf{a}_T(\phi_{p,k}^{(b)})^H \quad (5)$$

where $P^{(b)}$ is the number of signal paths and $\beta_{p,k}^{(b)}$ is the gain of path p which is distributed according to $\mathcal{CN}(0, F_k^{(b)})$. In the above, $F_k^{(b)}$ is the free space path loss, calculated as $F_k^{(b)} = (\lambda^{(b)}/4\pi d_k^{(b)})^2$, where $d_k^{(b)}$ is the distance between the BS b and user k . Also, $\theta_{p,k}^{(b)}$ and $\phi_{p,k}^{(b)}$ denote the angle of arrival (AoA) and angle of departure (AoD) for the p -th path between the BS and user k . The transmit and receive antenna array responses are given by $\mathbf{a}_T(\theta_{p,k}^{(b)}) = \frac{1}{\sqrt{N_t}} [1, e^{j\frac{2\pi s_t^{(b)}}{\lambda^{(b)}} \sin \theta_{p,k}^{(b)}}, \dots, e^{j(N_t-1)\frac{2\pi s_t^{(b)}}{\lambda^{(b)}} \sin \theta_{p,k}^{(b)}}]^T$ and $\mathbf{a}_R(\theta_{p,k}^{(b)}) = \frac{1}{\sqrt{N_k}} [1, e^{j\frac{2\pi s_k}{\lambda^{(b)}} \sin \phi_{p,k}^{(b)}}, \dots, e^{j(N_k-1)\frac{2\pi s_k}{\lambda^{(b)}} \sin \phi_{p,k}^{(b)}}]^T$, respectively, where $s_t^{(b)}$ and s_k are the spacing between the adjacent transmit and receive antennas, respectively.

For a single frequency band with bandwidth $B^{(b)}$, the achievable rate for user k can be expressed as

$$R_{C,k}^{(b)} = B^{(b)} \ln \det [\mathbf{I}_{N_k} + \mathbf{H}_k^{(b)} \mathbf{W}_k^{(b)} \mathbf{W}_k^{(b)H} \mathbf{H}_k^{(b)H} \times (\sum_{i=1, i \neq k}^K \mathbf{H}_k^{(b)} \mathbf{W}_i^{(b)} \mathbf{W}_i^{(b)H} \mathbf{H}_k^{(b)H} + (\sigma^{(b)})^2 \mathbf{I}_{N_k})^{-1}]. \quad (6)$$

B. Sensing Model

For target detection, each BS utilizes collocated transmit and receive antennas to perform monostatic sensing. We assume that the transmit and receive antennas at the same BS are separated and sufficiently isolated from one another, so that any self-interference can be ignored. Therefore, the AoD and AoA for each sensing signal are the same. If no scattering interference is present in the sensing channel, the echo signal is given by

$$\mathbf{Y}_S^{(b)} = \mathbf{G}^{(b)} \mathbf{X}^{(b)} + \mathbf{Z}^{(b)} = \mathbf{G}^{(b)} \mathbf{W}^{(b)} \mathbf{S}^{(b)} + \mathbf{Z}^{(b)} \quad (7)$$

where $\mathbf{G}^{(b)} \in \mathbb{C}^{N_r \times N_t}$ is the target response matrix and $\mathbf{Z}^{(b)} \in \mathbb{C}^{N_r \times L}$ is the noise matrix whose elements are distributed as $\mathcal{CN}(0, (\sigma^{(b)})^2)$. This equation can be further reformulated as [10]

$$\mathbf{y}_S^{(b)} = \widetilde{\mathbf{W}}^{(b)} \widetilde{\mathbf{g}}^{(b)} + \mathbf{z}^{(b)} \quad (8)$$

where $\widetilde{\mathbf{S}}^{(b)} = \mathbf{I}_{N_r} \otimes (\mathbf{S}^{(b)})^H$, $\widetilde{\mathbf{W}}^{(b)} = \mathbf{I}_{N_r} \otimes (\mathbf{W}^{(b)})^H$, $\mathbf{y}_S^{(b)} = \text{vec}((\mathbf{Y}_S^{(b)})^H)$, $\mathbf{g}^{(b)} = \text{vec}((\mathbf{G}^{(b)})^H)$ and $\mathbf{z}^{(b)} = \text{vec}((\mathbf{Z}^{(b)})^H)$.

For a point target, the response matrix and its covariance matrix are given by

$$\mathbf{G}^{(b)} = \alpha^{(b)} \sqrt{N_t N_r} \mathbf{a}_R(\varphi^{(b)}) \mathbf{a}_T(\varphi^{(b)})^H \quad (9)$$

$$\mathbf{R}^{(b)} = \mathbb{E}\{\mathbf{g}^{(b)} \mathbf{g}^{(b)H}\} = \gamma N_t N_r (\mathbf{a}_R(\varphi^{(b)})^* \otimes \mathbf{a}_T(\varphi^{(b)})) \times (\mathbf{a}_R(\varphi^{(b)})^* \otimes \mathbf{a}_T(\varphi^{(b)}))^H \quad (10)$$

where $\varphi^{(b)}$ is the sensing AoA/AoD, $\alpha^{(b)}$ is the reflection coefficient of the sensing channel gain, and $\gamma = \mathbb{E}\{\alpha^{(b)} \alpha^{(b)*}\}$. The standard deviation of $\alpha^{(b)}$ is $\sqrt{\beta_{\text{RCS}}(\lambda^{(b)})^2 / (4\pi)^3 (d^{(b)})^4}$, where $d^{(b)}$ is the distance between the BS and sensing target,

and β_{RCS} is the radar cross section (RCS) [11]. Since the proposed optimization algorithm is applicable for any RCS, we take $\beta_{\text{RCS}} = 1$ for ease of exposition. To enhance numerical stability, we normalize the communication channel and the target response matrices by the noise standard deviation, i.e., $\bar{\mathbf{H}}_k^{(b)} \leftarrow \mathbf{H}_k^{(b)}/\sigma^{(b)}$ and $\bar{\mathbf{G}}^{(b)} \leftarrow \mathbf{G}^{(b)}/\sigma^{(b)}$, which implies $\bar{\mathbf{R}}^{(b)} \leftarrow \mathbf{R}^{(b)}/(\sigma^{(b)})^2$.

For radar signal processing, both $\widetilde{\mathbf{W}}^{(b)}$ and $\widetilde{\mathbf{S}}^{(b)}$ are known to the receiver. Thus, the MI between $\mathbf{y}_S^{(b)}$ and $\mathbf{g}^{(b)}$ can be calculated as [10]

$$\begin{aligned} & \mathcal{I}(\mathbf{y}_S^{(b)}; \mathbf{g}^{(b)} | \widetilde{\mathbf{W}}^{(b)}, \widetilde{\mathbf{S}}^{(b)}) \\ &= \mathcal{H}(\mathbf{y}_S^{(b)} | \widetilde{\mathbf{W}}^{(b)}, \widetilde{\mathbf{S}}^{(b)}) - \mathcal{H}(\mathbf{y}_S^{(b)}; \mathbf{g}^{(b)} | \widetilde{\mathbf{W}}^{(b)}, \widetilde{\mathbf{S}}^{(b)}) \\ &= \ln \det(L \widetilde{\mathbf{W}}^{(b)} \bar{\mathbf{R}}^{(b)} (\widetilde{\mathbf{W}}^{(b)})^H + \mathbf{I}_{N_{\text{tot}} N_r}). \end{aligned} \quad (11)$$

From an information-theoretic point of view, we adopt the SR as the performance metric of sensing¹, which is defined as the sensing MI per unit time [13]. For target sensing at band b , the SR is given by

$$\begin{aligned} R_S^{(b)} &= \frac{1}{L} B^{(b)} \mathcal{I}(\mathbf{y}_S^{(b)}; \mathbf{g}^{(b)} | \widetilde{\mathbf{W}}^{(b)}, \widetilde{\mathbf{S}}^{(b)}) \\ &= \frac{1}{L} B^{(b)} \ln \det(L \widetilde{\mathbf{W}}^{(b)} \bar{\mathbf{R}}^{(b)} (\widetilde{\mathbf{W}}^{(b)})^H + \mathbf{I}_{N_{\text{tot}} N_r}). \end{aligned} \quad (12)$$

Note that both the CR in (6) and the SR in (12) are expressed in nats/s for mathematical convenience.

C. Problem Formulation

In this paper, we are interested in designing a cooperative ISAC system that maximizes the SR constrained by the total transmit power budget and the per-user CR requirements, leading to the following optimization problem:

$$\max_{\{\mathbf{W}_k^{(b)}\}} \sum_{b \in \mathcal{B}} R_S^{(b)} \quad (13a)$$

$$\text{s. t. } \sum_{b \in \mathcal{B}} \sum_{k=1}^K \text{Tr}(\mathbf{W}_k^{(b)} (\mathbf{W}_k^{(b)})^H) \leq P_{\text{max}}, \quad (13b)$$

$$\sum_{b \in \mathcal{B}} R_{C,k}^{(b)} \geq r_{\min}, \forall k \quad (13c)$$

where (13b) ensures the total transmit power does not exceed the maximum allowable power, and (13c) guarantees each user achieves at least the minimum required CR r_{\min} . Since we do not consider complex signal combining of the echo signals across different frequency bands, the sum SR serves as an appropriate objective function in (13).

III. PROPOSED SOLUTION

Since solving for $\{\mathbf{W}_k^{(b)}\}$ directly is challenging, we resort to the semi-definite rank relaxation method by introducing the covariance matrices $\mathbf{Q}_k^{(b)} = \mathbf{W}_k^{(b)} (\mathbf{W}_k^{(b)})^H$. As a result, the SR at band b can be rewritten as

$$\begin{aligned} R_S^{(b)} &= \frac{1}{L} B^{(b)} \ln \det(L \widetilde{\mathbf{W}}^{(b)} \bar{\mathbf{R}}^{(b)} (\widetilde{\mathbf{W}}^{(b)})^H + \mathbf{I}_{N_{\text{tot}} N_r}) \\ &= \frac{1}{L} B^{(b)} \ln \det[L(\mathbf{I}_{N_r} \otimes \sum_{k=1}^K \mathbf{Q}_k^{(b)}) \bar{\mathbf{R}}^{(b)} + \mathbf{I}_{N_t N_r}] \end{aligned} \quad (14)$$

where we used the identities $\det(\mathbf{X}\mathbf{Y} + \mathbf{I}_m) = \det(\mathbf{Y}\mathbf{X} + \mathbf{I}_n)$, $(\mathbf{X}_1 \mathbf{Y}_1) \otimes (\mathbf{X}_2 \mathbf{Y}_2) = (\mathbf{X}_1 \otimes \mathbf{X}_2)(\mathbf{Y}_1 \otimes \mathbf{Y}_2)$ and (1). We remark that $R_S^{(b)}$ is jointly concave with all $\mathbf{Q}_k^{(b)}$, which makes the objective function in (13a) easier to handle. Similarly, the CR of user k at band b is given by

$$R_{C,k}^{(b)} = B^{(b)} [\ln \det(\mathbf{B}_k^{(b)} + \bar{\mathbf{H}}_k^{(b)} \mathbf{Q}_k^{(b)} \bar{\mathbf{H}}_k^{(b)H}) - \ln \det(\mathbf{B}_k^{(b)})] \quad (15)$$

¹For the reason of consistency, the SR is chosen as the performance metric for sensing since we use the CR as the metric for communication. Alternatively, the MI can be used as the performance metric for both communication and sensing, as was done in [12].

where $\mathbf{B}_k^{(b)} = \sum_{j=1, j \neq k}^K \bar{\mathbf{H}}_k^{(b)} \mathbf{Q}_j^{(b)} \bar{\mathbf{H}}_k^{(b)H} + \mathbf{I}_{N_k}$. Therefore, the original optimization problem (13) can be equivalently reformulated as

$$\max_{\mathbf{Q}_k^{(b)} \in \mathcal{Q}} f(\{\mathbf{Q}_k^{(b)}\}) \triangleq \sum_{b \in \mathcal{B}} R_S^{(b)} \quad (16a)$$

$$\text{s. t. } \sum_{b \in \mathcal{B}} R_{C,k}^{(b)} \geq r_{\min}, \forall k \quad (16b)$$

$$\text{rank}(\mathbf{Q}_k^{(b)}) = N_k \quad (16c)$$

where $\mathcal{Q} \triangleq \{\mathbf{Q}_k^{(b)} | \sum_{b \in \mathcal{B}} \sum_{k=1}^K \text{Tr}(\mathbf{Q}_k^{(b)}) \leq P_{\text{max}}\}$ and (16c) ensures that $\mathbf{W}_k^{(b)}$ can be exactly computed from $\mathbf{Q}_k^{(b)}$.

It is straightforward to see that the primary challenges in solving (16) are the non-convex constraints (16b) and (16c). To overcome these, we drop the rank constraint (16c), and then apply the IA method to solve the resulting problem [14]. To this end, a concave lower bound for $R_{C,k}^{(b)}$ is required. We note that $R_{C,k}^{(b)}$ is in fact the difference of two concave functions. Thus, a lower bound can be easily obtained by linearizing the term $\ln \det(\mathbf{B}_k^{(b)})$. Let $\mathbf{Q}_k^{(b),n}$ and $\mathbf{B}_k^{(b),n}$ be the values of $\mathbf{Q}_k^{(b)}$ and $\mathbf{B}_k^{(b)}$ in the n -th iteration, respectively. Then the following inequality holds:

$$\begin{aligned} \ln \det(\mathbf{B}_k^{(b)}) &\leq \ln \det(\mathbf{B}_k^{(b),n}) + \\ &\sum_{i=1, i \neq k}^K \text{Tr}(\mathbf{H}_k^{(b)H} (\mathbf{B}_k^{(b),n})^{-1} \mathbf{H}_k^{(b)} (\mathbf{Q}_i^{(b)} - \mathbf{Q}_i^{(b),n})) \end{aligned} \quad (17)$$

which is due to the concavity of the $\ln \det(\cdot)$ function.

Substituting (17) into (15), a lower bound on the CR is given by

$$\begin{aligned} R_{C,k}^{(b)} &\geq \bar{R}_{C,k}^{(b)} = B^{(b)} \left[\ln \det(\mathbf{B}_k^{(b)} + \bar{\mathbf{H}}_k^{(b)} \mathbf{Q}_k^{(b)} \bar{\mathbf{H}}_k^{(b)H}) - \ln \det(\mathbf{B}_k^{(b),n}) \right. \\ &\quad \left. - \sum_{i=1, i \neq k}^K \text{Tr}(\bar{\mathbf{H}}_k^{(b)H} (\mathbf{B}_k^{(b),n})^{-1} \bar{\mathbf{H}}_k^{(b)} (\mathbf{Q}_i^{(b)} - \mathbf{Q}_i^{(b),n})) \right]. \end{aligned} \quad (18)$$

which is jointly concave with respect to all $\mathbf{Q}_k^{(b)}$. Utilizing (18), $\mathbf{Q}_i^{(b),n+1}$ is obtained as the solution to the following convex problem:

$$\max_{\mathbf{Q}_k^{(b)} \in \mathcal{Q}} f(\{\mathbf{Q}_k^{(b)}\}) \quad (19a)$$

$$\text{s. t. } \sum_{b \in \mathcal{B}} \bar{R}_{C,k}^{(b)} \geq r_{\min}, \forall k, \quad (19b)$$

Initialization: The proposed method requires a feasible point to start, which is not trivial to obtain due to the nonconvexity of $R_{C,k}^{(b)}$. To overcome this issue, we consider the following regularized problem of (19):

$$\max_{\mathbf{Q}_k^{(b)} \in \mathcal{Q}, s_k \geq 0} f(\{\mathbf{Q}_k^{(b)}\}) - \rho \sum_{k=1}^K s_k \quad (20a)$$

$$\text{s. t. } \sum_{b \in \mathcal{B}} \bar{R}_{C,k}^{(b)} + s_k \geq r_{\min}, \forall k \quad (20b)$$

where $s_k \geq 0$ ($k = 1, 2, \dots, K$) are slack variables, and $\rho > 0$ is the regularization parameter. It is straightforward to see that (20) is always feasible for any initial choice of $\mathbf{Q}_i^{(b),0}$. Due to the regularization term, the slack variables are gradually forced to zero as the iterations progress. Once this happens, the obtained $\mathbf{Q}_k^{(b)}$ is feasible to (16), and thus, can be used to initialize the proposed iterative optimization method. **Algorithm 1** outlines the overall proposed method.

Remark 1. After the optimization is complete, the appropriate precoding matrices $\mathbf{W}_k^{(b)}$ can be obtained from the covariance

Algorithm 1: Optimization of the covariance matrices.

Input: $\mathbf{Q}_k^{(b),0}$ (randomly generated), $\rho \geq 0$, $m \leftarrow 0$
repeat // find a feasible point
 2 Solve (20) to obtain $\mathbf{Q}_k^{(b),m+1}$ and increase m : $m \leftarrow m + 1$
 3 **until** $s_k < \epsilon (\forall k)$
 4 Reset $\mathbf{Q}_k^{(b),0} \leftarrow \mathbf{Q}_k^{(b),m+1}$ and set $n \leftarrow 0$
repeat
 6 Solve (19) to obtain $\mathbf{Q}_k^{(b),n+1}$ and increase n : $n \leftarrow n + 1$
 7 **until** convergence
Output: $\mathbf{Q}_k^{(b),*} = \mathbf{Q}_k^{(b),n+1}$, $k = 1, 2, \dots, K$

matrices $\mathbf{Q}_k^{(b),*}$. If $\text{rank}(\mathbf{Q}_k^{(b),*}) = N_k$, then $\mathbf{W}_k^{(b)}$ can be obtained exactly from $\mathbf{Q}_k^{(b),*}$ by eigenvalue decomposition (EVD). If not, then randomization methods introduced in [15] are applied to find $\mathbf{W}_k^{(b)}$. However, in our extensive numerical experiments, the condition $\text{rank}(\mathbf{Q}_k^{(b),*}) = N_k$ is always met, and thus, randomization is not necessary. This strongly suggests the potential existence of an analytical proof for this empirical observation. Pursuing such a proof is beyond the scope of this work, and we leave this interesting open problem for future research. For the high-frequency bands, $\mathbf{W}_{BB,k}^{(b)}$ and $\mathbf{W}_{RF,k}^{(b)}$ are obtained from $\mathbf{W}_k^{(b)}$ by applying orthogonal matching pursuit (OMP) [16, Algorithm 1].

Complexity Analysis: To analyze the computational complexity for solving (20), we have to transform it into a more standard form, which includes positive semidefinite (PSD) and exponential cones. To get a crude estimate of the complexity, we neglect the exponential cones, since the computational complexity is mostly dominated by the PSD cones and can be approximated by $\mathcal{O}(B^{3.5} N_r^{6.5} N_t^{6.5})$ [17, Section 6.6.3].

Convergence Analysis: The convergence analysis of the proposed method closely follows the arguments presented in [14]. It is easy to see that the inequality in (18) is tight when $\mathbf{Q}_i^{(b)} = \mathbf{Q}_i^{(b),n}$, $i = 1, 2, \dots, K$, which implies that $\{\mathbf{Q}_i^{(b),n}\}$ is feasible to (19). Since $\{\mathbf{Q}_i^{(b),n+1}\}$ is the global solution to (19), it follows that $f(\{\mathbf{Q}_i^{(b),n+1}\}) \geq f(\{\mathbf{Q}_i^{(b),n}\})$, i.e., the objective sequence $f(\{\mathbf{Q}_k^{(b),n}\})$ is nondecreasing. Assuming that the feasible set of (16) is nonempty, then the sequence $f(\{\mathbf{Q}_k^{(b),n}\})$ is bounded above, and is thus convergent since the feasible set is compact.

We remark that the objective function in (20a) strikes a balance between maximizing the SR and ensuring the feasibility of (19). Thus, once a feasible starting point is achieved (cf. Line 4 of **Algorithm 1**), it is also a good starting point. This, in turn, accelerates the convergence of the main iterative procedure, enabling the algorithm to terminate within only a few iterations, as shall be demonstrated in the next section.

IV. SIMULATION RESULTS

In this section, we evaluate the SR of the proposed algorithm for a cooperative ISAC system through Monte Carlo simulations and compare it with benchmark schemes. In the first benchmark scheme, which is denoted as *Eq-Pow-Split*, the total power budget is uniformly distributed among all BSs, i.e., the power budget of each BS is P_{\max}/B . In the other three benchmark schemes, which are denoted as *BS1 Only*, *BS2 Only* and *BS3 Only*, only the BS1, BS2 and BS3 are active, respectively.

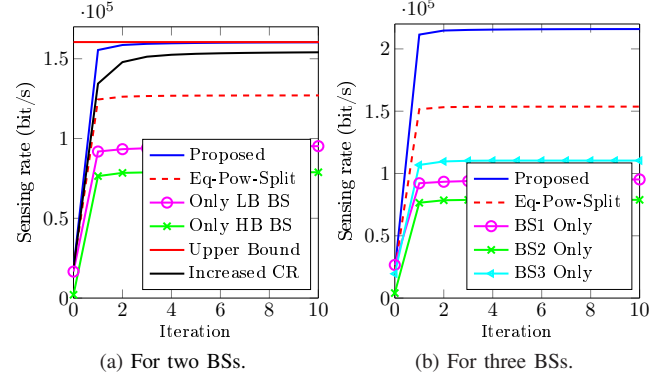


Fig. 1. Convergence of the proposed algorithm and of the benchmark schemes for different numbers of BSs.

In the simulation setup, we consider three frequency bands $f^{(1)} = 6$ GHz ($\lambda^{(1)} = 5$ cm), $f^{(2)} = 26$ GHz ($\lambda^{(2)} \approx 1.15$ cm), $f^{(3)} = 26.5$ GHz ($\lambda^{(3)} \approx 1.13$ cm) with corresponding bandwidths $B^{(1)} = 1$ MHz and $B^{(2)} = B^{(3)} = 4$ MHz. That is, BS1 operates in a low-frequency band, while BS2 and BS3 operate in a high-frequency bands. The number of propagation paths is $P^{(1)} = 8$ and $P^{(2)} = P^{(3)} = 4$, while the minimum communication rate requirement is $r_{\min} = 100$ kbits/s. Other parameters are set as $N_t = 8$, $N_r = 2$, $N_k = 2$, $P_{\max} = 0.1$ W, $L = 30$, $\rho = 1$, $\epsilon = 10^{-5}$. The noise power is calculated according to $(\sigma^{(b)})^2 = k_B T B^{(b)} F$, where $k_B = 1.381 \times 10^{-23}$ is the Boltzmann constant, $T = 290$ K is the standard temperature, and $F = 7.94$ (i.e., 9 dB) is the noise figure of the receiver. The midpoints of the transmit and the receive uniform linear arrays (ULAs) for BS1, BS2, and BS3 are at (0, 5 m, 0), (0, 5 m, 300 m), and (210 m, 5 m, -80 m), respectively, with ULAs at BS1 and BS2 oriented along the z -axis, and at BS3 along the x -axis. The midpoint of the k -th user's ULA is (25 m, 1.5 m, z_k), where z_k is uniformly distributed in [25 m, 275 m], while the point target is located at (-25 m, 1 m, z_t), where z_t follows the same uniform distribution as z_k . The inter-antenna spacing for each BS is half of the wavelength of its operating frequency, while for users, this spacing is $\lambda^{(1)}/2$ to avoid antenna coupling. The AoA ($\theta_{p,k}^{(b)}$) and AoD ($\phi_{p,k}^{(b)}$) are uniformly sampled from $[-\pi/2, \pi/2]$. The CVX tool with MOSEK as the internal software package is used to implement **Algorithm 1**. The initial values of the covariance matrices are randomly generated while satisfying the total power budget. **Algorithm 1** terminates once the relative change of the SR is less than 10^{-3} . Moreover, the SR is measured in bits per second (bits/s) and averaged over 500 independent channel realizations.

In Fig. 1, we present the convergence behavior of the proposed algorithm and of the benchmark schemes for a cooperative ISAC system with two and three BSs. In general, *all schemes require only a few iterations to fully converge after a feasible point is found*. Due to its ability to optimally distribute power among the BSs, the proposed algorithm achieves the largest SR, outperforming the *Eq-Pow-Split* scheme by approximately 25% and 40% in cooperative ISAC systems with two and three BSs, respectively. In addition, the proposed scheme achieves the same SR as the *Upper Bound*

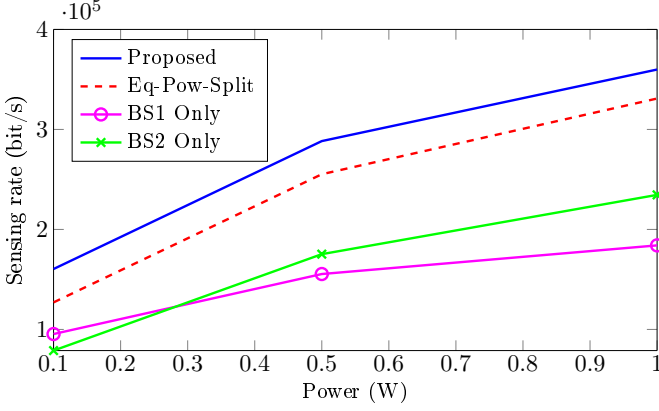


Fig. 2. Variations of the SR with the transmit power.

benchmark scheme, which excludes the CR constraint and therefore provides an upper bound on the achievable SR. The SR of *Upper Bound* can be obtained by using the water-filling algorithm. Furthermore, substantially increasing the minimum CR, r_{\min} , to 24 Mbit/s (i.e., the *Increased CR* benchmark scheme) causes a negligible reduction in the SR. The SRs of *Upper Bound* and *Increased CR* in a system with 3 BSs follow the same trend as in a system with 2 BSs, and thus, are omitted from Fig. 1(b) for the purpose of clarity. These results confirm the effectiveness of the proposed algorithm. Regarding benchmark schemes with only one active BS, *BS3 Only* achieves the highest individual SR, although it operates at a higher frequency than the other BSs. This can be attributed to the fact that the BS3 is in most cases closer to the sensing target, particularly when the target is equidistant from the first two BSs. These results indicate that, besides the operating frequency, the distance from the sensing target is another key factor that determines the SR in ISAC cooperative systems. In general, we can observe that the proposed algorithm for cooperative ISAC systems generally offers a substantially larger SR compared to benchmark schemes with only one active BS. Moreover, in our simulations, $\text{rank}(\mathbf{Q}_k^{(b),*})$ is always equal to N_k for $k = 1, 2, \dots, K$, which implies that dropping the rank constraint does not affect the optimality of (16).

The variation of the SR with the transmit power for the case of two BSs is shown in Fig. 2. Similar results were obtained for the case of three BSs. As expected, the SRs of all schemes increase logarithmically with the transmit power. The advantage of using the cooperative ISAC capabilities of both BSs, rather than relying on a single BS, becomes more apparent with higher transmit power. The proposed scheme consistently achieves a larger SR than *Eq-Pow-Split*, but the performance gap remains approximately constant across different power levels. This suggests that the proposed scheme is particularly beneficial in the low to medium transmit power range, while *Eq-Pow-Split* serves as an effective sub-optimal solution in the high transmit power regime. Regarding the benchmark schemes with only one active BS, *BS1 Only* achieves a larger SR in the lower transmit power region, while the opposite is true in the higher transmit power region. This is due to the fact that at higher transmit power levels, the higher propagation losses associated with higher-frequency bands (e.g., BS2) can be compensated by increased channel directivity, which

enhances sensing performance.

V. CONCLUSION

In this paper, we have studied the sum SR maximization in a cooperative ISAC system with linear precoding, where each BS operates in a different frequency band. With this aim, we developed an algorithm based on the semi-definite rank relaxation method by introducing the covariance matrices of the appropriate precoding matrices as optimization variables and utilized the IA method to deal with the nonconvexity of the resulting problem. Simulation results show that the proposed algorithm increases the SR by approximately 25 % and 40 % compared to the case of equal power distribution in a cooperative ISAC system with two and three BSs, respectively. Additionally, the algorithm converges in a couple of iterations. Lastly, we conclude that the proposed method is most effective in the low transmit power regime, where power-efficient cooperative sensing and communication are essential. Future work includes the evaluation of the proposed method under more advanced target models, including the incorporation of a clutter model.

REFERENCES

- [1] F. Liu *et al.*, "Integrated sensing and communications: Toward dual-functional wireless networks for 6G and beyond," *IEEE J. Sel. Areas Commun.*, vol. 40, no. 6, pp. 1728–1767, 2022.
- [2] A. Magbool *et al.*, "Multi-functional RIS for a multi-functional system: Integrating sensing, communication, and wireless power transfer," *IEEE Network*, vol. 39, no. 1, pp. 71–79, 2025.
- [3] C.-X. Wang *et al.*, "On the road to 6G: Visions, requirements, key technologies, and testbeds," *IEEE Commun. Surv. Tutor.*, vol. 25, no. 2, pp. 905–974, 2023.
- [4] S. Liu *et al.*, "Cooperative cell-free ISAC networks: Joint BS mode selection and beamforming design," in *Proc. IEEE WCNC*, 2024, pp. 1–6.
- [5] K. Meng *et al.*, "Cooperative ISAC networks: Performance analysis, scaling laws and optimization," *IEEE Trans. Wireless Commun.*, vol. 24, no. 2, pp. 877–892, 2025.
- [6] L. Pucci *et al.*, "Cooperative maximum likelihood target position estimation for MIMO-ISAC networks," *IEEE Wireless Commun. Lett.*, vol. 14, no. 5, pp. 1531–1535, 2025.
- [7] M. Liu *et al.*, "Performance analysis and power allocation for cooperative ISAC networks," *IEEE Internet Things J.*, vol. 10, no. 7, pp. 6336–6351, 2022.
- [8] H. Liu *et al.*, "Target localization with macro and micro base stations cooperative sensing," in *Proc. IEEE GLOBECOM*, 2024, pp. 1–6.
- [9] —, "Carrier aggregation enabled MIMO-OFDM integrated sensing and communication," *IEEE Trans. Wireless Commun.*, vol. 24, no. 6, pp. 4532–4548, 2025.
- [10] J. Li *et al.*, "A framework for mutual information-based MIMO integrated sensing and communication beamforming design," *IEEE Trans. Veh. Technol.*, vol. 73, no. 6, pp. 8352–8366, 2024.
- [11] F. Dong *et al.*, "Sensing as a service in 6G perceptive networks: A unified framework for ISAC resource allocation," *IEEE Trans. Wireless Commun.*, vol. 22, no. 5, pp. 3522–3536, 2022.
- [12] A. Bazzi and M. Chaffii, "Mutual information based pilot design for ISAC," *IEEE Trans. Commun.*, 2025, Early Access.
- [13] C. Ouyang *et al.*, "MIMO-ISAC: Performance analysis and rate region characterization," *IEEE Wireless Commun. Lett.*, vol. 12, no. 4, pp. 669–673, 2023.
- [14] B. R. Marks and G. P. Wright, "A general inner approximation algorithm for nonconvex mathematical programs," *Operations Research*, vol. 26, no. 4, pp. 681–683, 1978.
- [15] N. D. Sidiropoulos *et al.*, "Transmit beamforming for physical-layer multicasting," *IEEE Trans. Signal Process.*, vol. 54, no. 6, pp. 2239–2251, 2006.
- [16] O. El Ayach *et al.*, "Spatially sparse precoding in millimeter wave MIMO systems," *IEEE Trans. Wireless Commun.*, vol. 13, no. 3, pp. 1499–1513, 2014.
- [17] A. Ben-Tal and A. Nemirovski, *Lectures on modern convex optimization: analysis, algorithms, and engineering applications*. SIAM, 2001.